Simulations of solitary waves of RLW equation by exponential B-spline Galerkin method*

Melis Zorsahin Gorgulu[1,†], Idris Dag[2], and Dursun Irk[1]

[1] Department of Mathematics-Computer, Eskisehir Osmangazi University, 26480, Eskisehir, Turkey

[2] Department of Computer Engineering, Eskisehir Osmangazi University, 26480, Eskisehir, Turkey

(Received 13 January 2017; revised manuscript received 20 March 2017; published online 10 July 2017)

In this paper, an approximate function for the Galerkin method is composed using the combination of the exponential B-spline functions. Regularized long wave equation (RLW) is integrated fully by using an exponential B-spline Galerkin method in space together with Crank–Nicolson method in time. Three numerical examples related to propagation of single solitary wave, interaction of two solitary waves and wave generation are employed to illustrate the accuracy and the efficiency of the method. Obtained results are compared with some early studies.

Keywords: solitary waves, exponential B-spline, Galerkin method, RLW equation

PACS: 02.30.Jr, 02.70.Dh, 47.35.Fg, 04.30.Nk **DOI:** 10.1088/1674-1056/26/8/080202

1. Introduction

Peregrine puts forward to describing the nonlinear dispersive waves with small amplitude on the surface of water in a channel.[1] Since then, some physical phenomena such as nonlinear transverse waves in shallow water, ion-acoustic and magnetohydrodynamic waves in plasma, and phonon packets in nonlinear crystals are modelled by RLW equations. Since it has no analytical solutions generally, good numerical methods are needed to reveal physical events modelled by the regularized long wave equation (RLW) equation.

Many studies exist for the numerical solutions of the differential equations using splines. Splines are piecewise functions which have certain continuity at the joint points given to set up the splines. The spline related numerical techniques mainly offer the economical computer code and easy computational calculations. Thus they are preferable in forming the numerical methods. Until now, polynomial splines have been extensively developed and used for approximation of curve and surfaces and finding solutions of the differential equations. The polynomial spline based algorithms have been found to be quite advantageous for finding solutions of the differential equations. Base of splines known as the B-splines is also widely used to build up the trial functions for numerical methods. The exponential spline is proposed to be more general form of these splines. In the approximation theory, the exponential B-spline approximation is shown to model the data which have sudden growth and decay whereas polynomials are not appropriate due to having osculatory behavior. Since some differential equations have steep solutions, the use of the exponential B-splines in the numerical methods may exhibit good solutions for differential equations. McCartin[2] has introduced the exponential B-spline as a basis for the space of exponential splines. The exponential B-spline properties accord with those of polynomial B-splines such as smoothness, compact support, positivity, recursion for derivatives. Thus the exponential B-splines can be used as the trial function for the variational methods such as Galerkin and collocation methods.

The exponential B-spline based methods have been started to solve some differential equations: Numerical solution of the singular perturbation problem is solved with a variant of exponential B-spline collocation method in Ref. [3], the cardinal exponential B-splines is used for solving the singularly perturbed problems,[4] the exponential B-spline collocation method is built up for finding the numerical solutions of the self-adjoint singularly perturbed boundary value problems in Ref. [5], the numerical solutions of the convection–diffusion equation is obtained by using the exponential B-spline collocation method.[6] Recently, a collocation method based on the exponential B-splines has been set up to find numerical solutions of the Fisher equation, generalized Burgers–Fisher equation and RLW equation.[7–9] In this study, the combination of the exponential B-splines are used to form the trial function for the Galerkin method which is known to produce the smaller error for solutions of the differential equations. The RLW equation will be solved with the proposed exponential B-spline Galerkin method over the problem domain. Newly, a study in which the exponential B-splines are adapted to the Galerkin method to have solutions of the Burgers equation has appeared.[10] Thus we want to see the efficiency of the exponential B-spline Galerkin method for the RLW equation.

*Project supported by the Scientific and Technological Research Council of Turkey (Grant No. 113F394).

†Corresponding author. E-mail: mzorsahin@ogu.edu.tr

© 2017 Chinese Physical Society and IOP Publishing Ltd

The RLW equation describes a large number of important physical phenomena, such as shallow waters and plasma waves. Therefore it plays a major role in the study of nonlinear dispersive waves. Because of having limited analytical solutions, numerical analysis of the RLW equation has an importance in its study. Various techniques have been developed to obtain the numerical solution of the RLW equation, some of which are finite difference methods,[1,11–14] finite element methods,[15–25] and spectral methods.[26–28] Spline functions are adapted to some of these standard methods to construct spline-related algorithms.

The paper is outlined as follows. In Section 2, exponential B-splines and their some basic relations are introduced. In Section 3, the application of the numerical method is given. The efficiency and the accuracy of the present method are investigated by using three numerical experiments related to propagation of single solitary wave, interaction of two solitary waves and wave generation. Finally some remarks are concluded in the last section.

2. Exponential B-splines and finite element solution

In this study, we will consider the RLW equation

$$u_t + u_x + \varepsilon u u_x - \mu u_{xxt} = 0, \tag{1}$$

where x is space coordinate, t is time, u is the wave amplitude, and ε and μ are positive parameters. Boundary and initial conditions of Eq. (1) are

$$\begin{aligned} &u(a,t) = \beta_1, && u(b,t) = \beta_2, \\ &u_x(a,t) = 0, && u_x(b,t) = 0,\ t \in (0,T], \\ &u(x,0) = f(x), && x \in [a,b]. \end{aligned} \tag{2}$$

The equation (1) was first introduced by Peregrine[1] for modelling the propagation of unidirectional weakly nonlinear and weakly dispersive water waves. Since the RLW equation obviates the certain problematical aspects of KdV equation and it generally has more expedient mathematical properties, Benjamin *et al.*[29] proposed the use of the RLW equation as a preferable model to the KdV equation.

Let us consider a uniform mesh Γ with the knots x_i on $[a,b]$ such that

$$\Gamma : a = x_0 < x_1 < x_2 < \cdots < x_{N-1} < x_N = b,$$

where $h = (b-a)/N$ and $x_i = x_0 + \mathrm{i}h$.

Let $\phi_i(x)$ be the B-splines at the points of Γ together with knots x_i, $i = -3,-2,-1,N+1,N+2,N+3$ outside the interval $[a,b]$ and having a finite support on the four consecutive intervals $[x_i + kh, x_i + (k+1)h]_{k=-3}^{0}$, $i = 0,\ldots,N+2$. The $\phi_i(x)$ can be defined as

$$\phi_i(x) = \begin{cases} b_2\left[(x_{i-2}-x) - \dfrac{1}{p}\left(\sinh\left(p\left(x_{i-2}-x\right)\right)\right)\right], & \text{if } x \in [x_{i-2}, x_{i-1}]; \\ a_1 + b_1(x_i - x) + c_1 \mathrm{e}^{p(x_i-x)} + d_1 \mathrm{e}^{-p(x_i-x)}, & \text{if } x \in [x_{i-1}, x_i]; \\ a_1 + b_1(x - x_i) + c_1 \mathrm{e}^{p(x-x_i)} + d_1 \mathrm{e}^{-p(x-x_i)}, & \text{if } x \in [x_i, x_{i+1}]; \\ b_2\left[(x-x_{i+2}) - \dfrac{1}{p}\left(\sinh\left(p\left(x-x_{i+2}\right)\right)\right)\right], & \text{if } x \in [x_{i+1}, x_{i+2}]; \\ 0, & \text{otherwise.} \end{cases} \tag{3}$$

where

$$\begin{aligned} p &= \max_{0\le i\le N} p_i, \quad s = \sinh(ph), \quad c = \cosh(ph), \\ a_1 &= \frac{phc}{phc - s}, \\ b_1 &= \frac{p}{2}\left[\frac{c(c-1) + s^2}{(phc-s)(1-c)}\right], \\ b_2 &= \frac{p}{2(phc-s)}, \\ c_1 &= \frac{1}{4}\left[\frac{\mathrm{e}^{-ph}(1-c) + s\left(\mathrm{e}^{-ph}-1\right)}{(phc-s)(1-c)}\right], \\ d_1 &= \frac{1}{4}\left[\frac{\mathrm{e}^{ph}(c-1) + s\left(\mathrm{e}^{ph}-1\right)}{(phc-s)(1-c)}\right]. \end{aligned}$$

Each basis function $\phi_i(x)$ is twice continuously differentiable. The values of $\phi_i(x)$, $\phi_i'(x)$, and $\phi_i''(x)$ at the knots x_i's are obtained from Table 1.

Table 1. Exponential B-spline values.

	x_{i-2}	x_{i-1}	x_i	x_{i+1}	x_{i+2}
$\phi_i(x)$	0	$\dfrac{s-ph}{2(phc-s)}$	1	$\dfrac{s-ph}{2(phc-s)}$	0
$\phi_i'(x)$	0	$\dfrac{p(c-1)}{2(phc-s)}$	0	$\dfrac{p(1-c)}{2(phc-s)}$	0
$\phi_i''(x)$	0	$\dfrac{p^2 s}{2(phc-s)}$	$\dfrac{-p^2 s}{phc-s}$	$\dfrac{p^2 s}{2(phc-s)}$	0

The $\phi_i(x)$, $i = -1,\ldots,N+1$ form a basis for functions defined on the interval $[a,b]$. We seek an approximation $U(x,t)$ to the analytical solution $u(x,t)$ in terms for the exponential

B-splines

$$u(x,t) \approx U(x,t) = \sum_{i=-1}^{N+1} \phi_i(x)\,\delta_i(t), \tag{4}$$

where $\delta_i(t)$ are time-dependent unknown to be determined from the boundary conditions and Galerkin approach to Eq. (1). The approximate solution and their derivatives at the knots can be found from Eqs. (3) and (4) as

$$\begin{aligned} U_i &= U(x_i,t) = \alpha_1\delta_{i-1} + \delta_i + \alpha_1\delta_{i+1},\\ U_i' &= U'(x_i,t) = \alpha_2\delta_{i-1} - \alpha_2\delta_{i+1},\\ U_i'' &= U''(x_i,t) = \alpha_3\delta_{i-1} - 2\alpha_3\delta_i + \alpha_3\delta_{i+1}, \end{aligned} \tag{5}$$

where

$$\begin{aligned} \alpha_1 &= (s-ph)/2(phc-s),\\ \alpha_2 &= p(1-c)/2(phc-s),\\ \alpha_3 &= p^2 s/2(phc-s). \end{aligned}$$

Applying the Galerkin method to the RLW equation with the exponential B-splines as weight function over the element $[a,b]$ gives

$$\int_a^b \phi_i(x)\,(u_t + u_x + \varepsilon u u_x - \mu u_{xxt})\,\mathrm{d}x = 0. \tag{6}$$

The approximate solution U over the element $[x_m, x_{m+1}]$ can be written as

$$\begin{aligned} U^{\mathrm{e}} = {}& \phi_{m-1}(x)\,\delta_{m-1}(t) + \phi_m(x)\,\delta_m(t)\\ & + \phi_{m+1}(x)\,\delta_{m+1}(t) + \phi_{m+2}(x)\,\delta_{m+2}(t), \end{aligned} \tag{7}$$

where quantities $\delta_j(t)$, $j = m-1,\ldots,m+2$ are element parameters and $\phi_j(x)$, $j = m-1,\ldots,m+2$ are known as the element shape functions.

The contribution of the integral equation (6) over the sample interval $[x_m, x_{m+1}]$ is given by

$$\int_{x_m}^{x_{m+1}} \phi_j(x)\,(u_t + u_x + \varepsilon u u_x - \mu u_{xxt})\,\mathrm{d}x. \tag{8}$$

Applying the Galerkin discretization scheme by replacing approximate solution U^{e} (7) and its derivatives U_t, U_x, U_{xxt} into the exact solution u and its derivatives u_t, u_x, u_{xxt} respectively, we obtain a system of equations in the unknown parameters δ_j

$$\sum_{i=m-1}^{m+2} \left\{ \left(\int_{x_m}^{x_{m+1}} \phi_j\phi_i\,\mathrm{d}x \right) \dot{\delta}_i + \left(\int_{x_m}^{x_{m+1}} \phi_j\phi_i'\,\mathrm{d}x \right) \delta_i + \varepsilon \left(\int_{x_m}^{x_{m+1}} \phi_j \left(\sum_{k=m-1}^{m+2} \delta_k\phi_k \right) \phi_i'\,\mathrm{d}x \right) \delta_i - \mu \left(\int_{x_m}^{x_{m+1}} \phi_j\phi_i''\,\mathrm{d}x \right) \dot{\delta}_i \right\}, \tag{9}$$

where i, j and k take only the values $m-1$, m, $m+1$, $m+2$ for $m = 0,1,\ldots,N-1$ and $\dot{}$ denotes time derivative.

In the above system of differential equations, when $\boldsymbol{A}^{\mathrm{e}}$, $\boldsymbol{B}^{\mathrm{e}}$, $\boldsymbol{C}^{\mathrm{e}}(\boldsymbol{\delta})$, and $\boldsymbol{D}^{\mathrm{e}}$ are denoted by

$$\begin{aligned} \boldsymbol{A}^{\mathrm{e}} &= \int_{x_m}^{x_{m+1}} \phi_j\phi_i\,\mathrm{d}x,\\ \boldsymbol{B}^{\mathrm{e}} &= \int_{x_m}^{x_{m+1}} \phi_j\phi_i'\,\mathrm{d}x,\\ \boldsymbol{C}^{\mathrm{e}}(\boldsymbol{\delta}) &= \int_{x_m}^{x_{m+1}} \phi_j \left(\sum_{k=m-1}^{m+2} \delta_k\phi_k \right) \phi_i'\,\mathrm{d}x,\\ \boldsymbol{D}^{\mathrm{e}} &= \int_{x_m}^{x_{m+1}} \phi_j\phi_i''\,\mathrm{d}x, \end{aligned} \tag{10}$$

where $\boldsymbol{A}^{\mathrm{e}}$, $\boldsymbol{B}^{\mathrm{e}}$, and $\boldsymbol{D}^{\mathrm{e}}$ are the element matrices of which dimensions are 4×4 and $\boldsymbol{C}^{\mathrm{e}}(\boldsymbol{\delta})$ is the element matrix with the dimension $4\times4\times4$, the matrix form of Eq. (9) can be written as

$$(\boldsymbol{A}^{\mathrm{e}} - \mu\boldsymbol{D}^{\mathrm{e}})\,\dot{\boldsymbol{\delta}}^{\mathrm{e}} + (\boldsymbol{B}^{\mathrm{e}} + \varepsilon\boldsymbol{C}^{\mathrm{e}}(\boldsymbol{\delta}^{\mathrm{e}}))\,\boldsymbol{\delta}^{\mathrm{e}}, \tag{11}$$

where

$$\boldsymbol{\delta}^{\mathrm{e}} = (\delta_{m-1},\ldots,\delta_{m+2})^{\mathrm{T}}.$$

Gathering the systems (11) over all elements, we obtain global system

$$(\boldsymbol{A} - \mu\boldsymbol{D})\,\dot{\boldsymbol{\delta}} + (\boldsymbol{B} + \varepsilon\boldsymbol{C}(\boldsymbol{\delta}))\,\boldsymbol{\delta} = 0, \tag{12}$$

where $\boldsymbol{A}$, $\boldsymbol{B}$, $\boldsymbol{C}(\boldsymbol{\delta})$, $\boldsymbol{D}$ are derived from the corresponding element matrices $\boldsymbol{A}^{\mathrm{e}}$, $\boldsymbol{B}^{\mathrm{e}}$, $\boldsymbol{C}^{\mathrm{e}}(\boldsymbol{\delta})$, $\boldsymbol{D}^{\mathrm{e}}$, respectively and

$$\boldsymbol{\delta} = (\delta_{-1},\ldots,\delta_{N+1})^{\mathrm{T}}$$

contain all elements parameters.

The unknown parameters $\boldsymbol{\delta}$ are interpolated between two time levels n and $n+1$ with the Crank–Nicolson method

$$\begin{aligned} \boldsymbol{\delta} &= \frac{\boldsymbol{\delta}^{n+1} + \boldsymbol{\delta}^n}{2},\\ \dot{\boldsymbol{\delta}} &= \frac{\boldsymbol{\delta}^{n+1} - \boldsymbol{\delta}^n}{\Delta t}, \end{aligned}$$

we obtain iterative formula for the time parameters $\boldsymbol{\delta}^n$

$$\left[(\boldsymbol{A} - \mu\boldsymbol{D}) + \frac{\Delta t}{2} \left(\boldsymbol{B} + \varepsilon\boldsymbol{C}\left(\boldsymbol{\delta}^{n+1}\right) \right) \right] \boldsymbol{\delta}^{n+1} = \left[(\boldsymbol{A} - \mu\boldsymbol{D}) - \frac{\Delta t}{2} (\boldsymbol{B} + \varepsilon\boldsymbol{C}(\boldsymbol{\delta}^n)) \right] \boldsymbol{\delta}^n. \tag{13}$$

The set of equations consist of $(N+3)$ equations with $(N+3)$ unknown parameters. Before starting the iteration procedure, boundary conditions must be adapted into the system and initial vector $\boldsymbol{\delta}^0$ must also be determined.

We delete first and last equations from system (13) and eliminate the terms δ_{-1}^{n+1} and δ_{N+1}^{n+1} from system (13) by using boundary conditions in Eq. (2), which give the following equations:

$$u(a,t) = \alpha_1\delta_{-1}^{n+1} + \delta_0^{n+1} + \alpha_1\delta_1^{n+1} = \beta_1,$$
$$u(b,t) = \alpha_1\delta_{N-1}^{n+1} + \delta_N^{n+1} + \alpha_1\delta_{N+1}^{n+1} = \beta_2.$$

We obtain a septa-diagonal matrix with the dimension $(N+1)\times(N+1)$. Then we can solve this matrix system through Thomas algorithm. Since system (13) is an implicit system due to the term $C\left(\boldsymbol{\delta}^{n+1}\right)$, we have used the following inner iteration:

$$(\boldsymbol{\delta}^*)^{n+1} = \boldsymbol{\delta}^{n+1} + \frac{(\boldsymbol{\delta}^{n+1} - \boldsymbol{\delta}^n)}{2}. \tag{14}$$

In this iteration, before moving the calculation of the next time step approximation for time parameter, we calculate the new vectors $(\boldsymbol{\delta}^*)^{n+1}$ using formula (14) from previous vectors $\boldsymbol{\delta}^{n+1}$ finding form the system (13) and then repeat three times at all time steps.

To start evolution of the vector of initial parameters $\boldsymbol{\delta}^0$, it must be determined by using the initial condition and boundary conditions

$$u'(x_0,0) = \frac{p(1-c)}{2(phc-s)}\delta_{-1} + \frac{p(c-1)}{2(phc-s)}\delta_1,$$
$$u(x_m,0) = \frac{s-ph}{2(phc-s)}\delta_{m-1} + \delta_m + \frac{s-ph}{2(phc-s)}\delta_{m+1},$$
$$m = 0,\ldots,N,$$
$$u'(x_N,0) = \frac{p(1-c)}{2(phc-s)}\delta_{N-1} + \frac{p(c-1)}{2(phc-s)}\delta_{N+1}. \tag{15}$$

The solution of matrix equation (15) with the dimensions $(N+3)\times(N+3)$ is obtained by the way of Thomas algorithm. Once $\boldsymbol{\delta}^0$ is determined, we can start the iteration of the system to find the parameters $\boldsymbol{\delta}^n$ at time $t^n = n\Delta t$. Approximate solutions at the knots is found from Eq. (5) and solution over the intervals $[x_m, x_{m+1}]$ is determined from Eq. (7).

To investigate the stability of system of the difference scheme (13), we apply the von Neumann stability analysis. A typical member of the linearized equation corresponding to Eq. (13) is given by

$$\gamma_1\delta_{m-3}^{n+1} + \gamma_2\delta_{m-2}^{n+1} + \gamma_3\delta_{m-1}^{n+1} + \gamma_4\delta_m^{n+1} + \gamma_5\delta_{m+1}^{n+1} + \gamma_6\delta_{m+2}^{n+1} + \gamma_7\delta_{m+3}^{n+1} = \gamma_7\delta_{m-3}^n + \gamma_6\delta_{m-2}^n + \gamma_5\delta_{m-1}^n + \gamma_4\delta_m^n + \gamma_3\delta_{m+1}^n + \gamma_2\delta_{m+2}^n + \gamma_1\delta_{m+3}^n,$$

where the parameters γ_i, $i = 1,\ldots,7$ are determined from system (13), in which these values are not preferred to document here due to being too long.

Substituting the Fourier mode $\delta_m^n = s^n\mathrm{e}^{\mathrm{i}m\varphi}$ into the linearized form of the difference equation becomes

$$s^{n+1} = qs^n.$$

Here, the growth factor is determined as

$$q = \frac{\hat{a} - \mathrm{i}\hat{b}}{\hat{a} + \mathrm{i}\hat{b}},$$

where

$$\hat{a} = (\gamma_1+\gamma_7)\cos(3\varphi) + (\gamma_2+\gamma_6)\cos(2\varphi) + (\gamma_3+\gamma_5)\cos(\varphi) + (\gamma_4),$$
$$\hat{b} = (\gamma_1-\gamma_7)\sin(3\varphi) + (\gamma_2-\gamma_6)\sin(2\varphi) + (\gamma_3-\gamma_5)\sin(\varphi).$$

Since the magnitude of the growth factor is $|q| = 1$, the difference scheme (13) is unconditionally stable.

3. Test problems

We have carried out three test problems to demonstrate the given algorithm. Accuracy of the method is measured by the error norm:

$$L_\infty = \left\|u^{\text{exact}} - u^{\text{numeric}}\right\|_\infty = \max_{0\le j\le N}\left|u_j^{\text{exact}} - u_j^{\text{numeric}}\right|.$$

The RLW equation satisfies the following conservation laws which are corresponding to mass, momentum, and energy:[30]

$$C_1 = \int_{-\infty}^{+\infty} u\,\mathrm{d}x,$$
$$C_2 = \int_{-\infty}^{+\infty}\left(u^2 + \mu(u_x)^2\right)\mathrm{d}x,$$
$$C_3 = \int_{-\infty}^{+\infty}\left(u^3 + 3u^2\right)\mathrm{d}x.$$

In numerical calculations, the conservation laws are calculated by use of the trapezoidal rule and the determination of p in the exponential B-spline is found by scanning the predetermined interval with a small increment experimentally in a way that the best numerical solutions are obtained for the test problems.

3.1. Propagation of single solitary wave

The exact solution of RLW equation is given in Ref. [1] as follows:

$$u(x,t) = \frac{3c}{\cosh^2\left(k\left(x - x_0 - (1+\varepsilon c)t\right)\right)}, \tag{16}$$

where

$$k = \frac{1}{2}\sqrt{\frac{\varepsilon c}{\mu\,(1+\varepsilon c)}}.$$

This form of the solution is known as a single solitary wave with the amplitude $3c$ and the velocity $1+\varepsilon c$. The initial condition is obtained by taking $t = 0$ in Eq. (16). We have used boundary conditions $\beta_1 = 0$, $\beta_2 = 0$. The values of the parameters seen in the above equations are

$$c = 0.1 \text{ and } 0.03,\ x_0 = 0,\ \varepsilon = 1,\ \mu = 1.$$

With these parameters and the mentioned initial condition, the solitary wave moves across the interval $-40 \le x \le 60$ in time period $0 \le t \le 20$. Similar with some early studies, space step $h = 0.125$ and time step $\Delta t = 0.1$ are used in numerical calculations. In this test problem, the $p = 0.01262$ is determined by scanning the interval $[0, 80]$ with the increment 0.1 first, then according to the results scanning the interval $[0, 1]$ with the increment 10^{-5}. The solution profiles are illustrated in Fig. 1 at selected times. It is clear from this figure that the peak of the solitary wave remain kept during the running time.

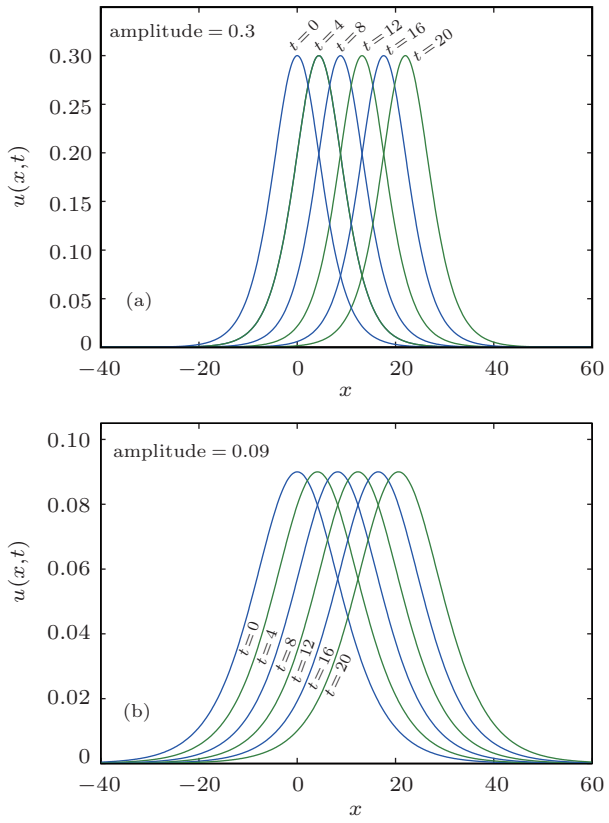


Fig. 1. (color online) Solitary wave solutions.

The distribution of the absolute error at $t = 20$ for amplitudes 0.3 and 0.09 is given in Figs. 2(a) and 2(b), respectively. The maximum error for the EBSGM occurs at the right hand boundary as shown in Fig. 2(b). We believe that this error arises due to magnitude of the wave and the physical boundary conditions to fit $u(a,0) \approx 0$ and $u(b,20) \approx 0$. If we extend the solution interval from $[-40, 60]$ to $[-80, 120]$, L_∞ error norm is seen to reduce from 0.4315×10^{-3} to 0.63035×10^{-5} at time $t = 20$.

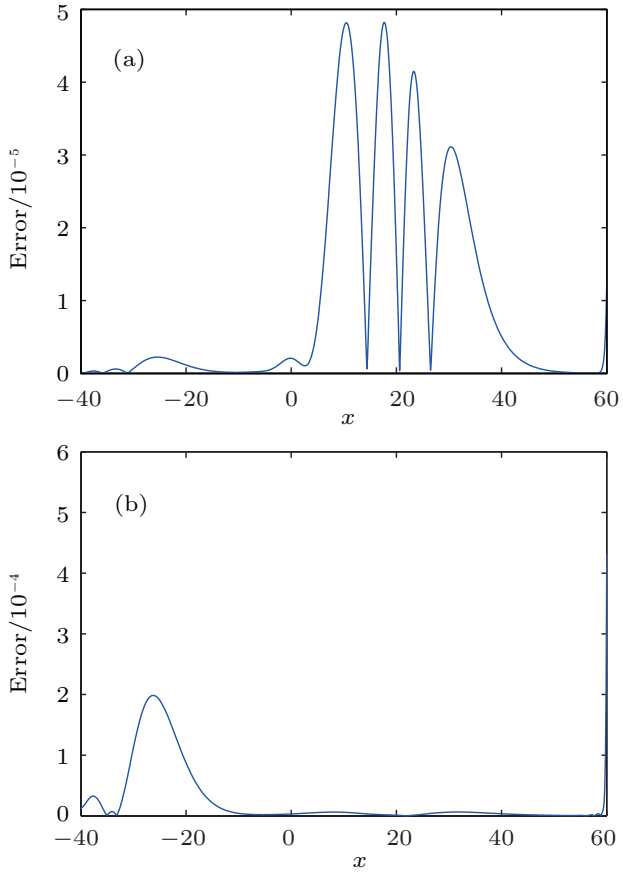


Fig. 2. (color online) The distribution of absolute error at $t = 20$ for (a) amplitude= 0.3, (b) amplitude= 0.09.

The absolute error norms and the values of the conservation invariants C_1, C_2, and C_3 are recorded in Tables 2 and 3 for different amplitudes, respectively. To make a comparison with some early studies, the maximum errors with the conservation invariants are presented in Table 4 and Table 5. According to these tables, the EBSGM gives more accurate results than or similar to some others except for the method of collocation accompanied with the exponential B-splines. The values of the conservation invariants C_1, C_2, and C_3 at different times remain fairly the same when compared with the analytical invariants $C_1 = 3.9799297$, $C_2 = 0.81046249$, $C_3 = 2.579007$ for amplitude 0.3. When we take the amplitude as 0.09, the value of the conservation invariant C_1 has some minor difference than the analytical value of it, whereas C_2 and C_3 are fairly same at different times.

Table 2. Errors and Invariants for amplitude $3c = 0.3$, $h = 0.125$, $\Delta t = 0.1$, $p = 0.01262$.

Time	$L_\infty \times 10^5$	C_1	C_2	C_3
0	0.000	3.9799267	0.8104625	2.5790074
4	1.268	3.9799299	0.8104625	2.5790075
8	2.445	3.9799281	0.8104625	2.5790076
12	3.418	3.9799255	0.8104626	2.5790077
16	4.197	3.9799168	0.8104626	2.5790078
20	4.820	3.9798827	0.8104626	2.5790079

Table 3. Errors and Invariants for amplitude $3c = 0.09$, $h = 0.125$, $\Delta t = 0.1$, $p = 0.01262$.

Time	$L_\infty \times 10^4$	C_1	C_2	C_3
0	0.000	2.1070467	0.1273013	0.3888047
4	2.302	2.1070975	0.1273011	0.3888041
8	2.214	2.1068946	0.1273011	0.3888041
12	2.129	2.1065454	0.1273011	0.3888040
16	2.139	2.1053719	0.1273012	0.3888032
20	4.315	2.1045885	0.1273012	0.3888023

Table 4. Errors and Invariants for amplitude $3c = 0.3$, $h = 0.125$, $\Delta t = 0.1$, $p = 0.01262$.

Method	Time	$L_\infty \times 10^3$	C_1	C_2	C_3
Analytical			3.97995	0.8104624	2.579007
EBSGM	20	0.04820	3.979883	0.8104626	2.579008
Ref. [9]	20	0.007743	3.979908	0.8104625	2.5790074
Ref. [24]	20	0.02643	3.979909	0.8104625	2.579007
Ref. [22]	20	0.07337	3.979883	0.8104612	2.579003
Ref. [21]	20	1.56640	3.961597	0.804185	2.558292
Ref. [23]	20	0.10299	3.979858	0.8104596	2.578999
Ref. [18]	20	0.116	3.979883	0.8102762	2.578393
Ref. [25]	20	0.91465	3.97972	0.81026	2.57873
Ref. [19]	20	0.07344	3.979888	0.8104622	2.579006
Ref. [20]	20	0.073	3.97989	0.81046	2.57901

Table 5. Errors and Invariants for amplitude $3c = 0.09$, $h = 0.125$, $\Delta t = 0.1$, $p = 0.01262$.

Method	Time	$L_\infty \times 10^3$	C_1	C_2	C_3
Analytical			2.109407	0.12730171	0.3888059
EBSGM	20	0.431512	2.104589	0.12730121	0.3888023
Ref. [9]	20	0.004174	2.107035	0.12730152	0.3888043
Ref. [21]	20	1.5506	2.128869	0.127228	0.388571
Ref. [18]	20	0.432	2.104584	0.12729366	0.3887776
Ref. [25]	20	0.439145	2.10902	0.12730	0.38880
Ref. [19]	20	0.19806	2.104708	0.1273006	0.3888025
Ref. [20]	20	0.199	2.10467	0.12730	0.38880

3.2. Interaction of two solitary waves

In this section, we will study the interaction of two solitary waves having different amplitudes and moving in the same direction. The initial condition is

$$u(x,0) = u_1 + u_2,$$
$$u_j = \frac{3A_j}{\cosh^2\left(k_j\left(x - \widetilde{x}_j\right)\right)},$$
$$A_j = \frac{4k_j^2}{1-4k_j^2},\ j = 1,2,$$

where the following parameters are chosen to coincide values in the literature

$$\varepsilon = 1,\ \ \mu = 1,\ \ k_1 = 0.4,\ \ k_2 = 0.3,$$
$$\widetilde{x}_1 = 15,\ \ \widetilde{x}_2 = 35,\ \ \beta_1 = 0,\ \ \beta_2 = 0.$$

Initially, these parameters yield the solitary waves with the amplitudes 5.333375 and 1.687502 positioning around points $x = 15$ and $x = 35$ respectively. The computation is carried out up to time $t = 30$ with time step $\Delta t = 0.1$, $N = 400$ over the finite interval $[0, 120]$ and p is selected as 1 for EBSGM.

Numerical solutions of $u(x,t)$ at various times are depicted in Fig. 3, and the initial solution has been propagated rightward. It is seen from Fig. 3 that the solitary waves are subjected to a collision about time $t = 15$ and after the interaction they propagate with their original amplitudes to the right seeing at time $t = 30$.

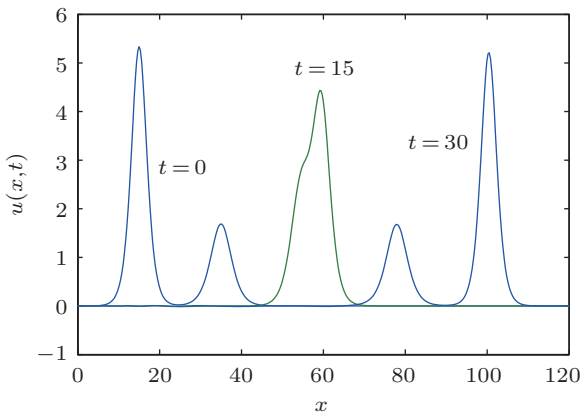


Fig. 3. (color online) Interaction of two positive solitary waves at $t = 0$, 15 and 30.

The conservation invariants are presented at some selected times in Table 6. According to this table, during the interaction there are some changes at the conservation constants C_2 and C_3 whereas the constant C_1 remain nearly the same.

Table 6. Invariants for $h = 0.3$, $\Delta t = 0.1$, and $p = 1$.

Time	C_1	C_2	C_3
0	37.916502	120.522247	744.081209
5	37.861378	119.772286	737.819263
10	37.810403	119.129874	732.319072
15	37.790851	119.012803	730.931470
20	37.752779	118.312087	725.698903
25	37.701304	117.600957	719.868731
30	37.650120	116.909863	714.174760

3.3. Wave generation

An applied force like an introduction of fluid mass, an action of some mechanical device, to a free surface, will induce waves. In this numerical experiment, we take following boundary condition to generate waves with the RLW equation.

$$u(a,t)=\beta_1=\begin{cases} U_0\dfrac{t}{\tau}, & 0\le t\le \tau,\\ U_0, & \tau<t<t_0-\tau,\\ U_0\dfrac{t_0-t}{\tau}, & t_0-\tau\le t\le t_0,\\ 0, & \text{otherwise.}\end{cases}$$

and $u(b,t)=\beta_2=0$ is studied to generate waves. This forced boundary condition known as a wave maker at one end.

The parameters $U_0=2, \Delta t=0.1, h=0.4, t_0=20, \tau=0.3$ are chosen to make a comparison with earlier works over the region $0\le x\le 260$. p is selected as 1 for EBSGM. During the run time of the algorithm, five solitary waves are produced. Although first four waves have reached amplitudes larger than forcing amplitudes, the last one is less than that of the forcing one. When forcing is switched off, the last wave has not enough time to evolve. Subsequently, no new wave is born. A view of travelling solitary wave is presented at time $t=100$ in Fig. 4. Amplitudes of solitary waves versus time are depicted in Fig. 5. At various time, amplitudes of the solitary waves and the conservation constants are demonstrated in Table 7 for EBSGM. In addition to this, other amplitudes of the solitary waves which are reduced the other studies are shown in Table 7 for time $t=100$. Our results are in conformity with that of studies[20,31,32]

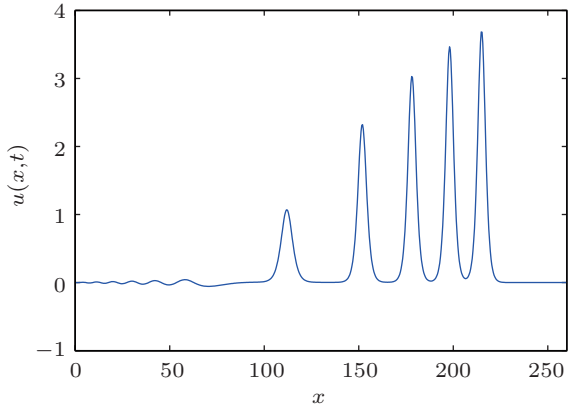


Fig. 4. (color online) Solitary wave produced by boundary forcing of duration $t_0=20$ and amplitude $U_0=2$ at time $t=100$, $h=0.4$, $\Delta t=0.1$, $p=1$.

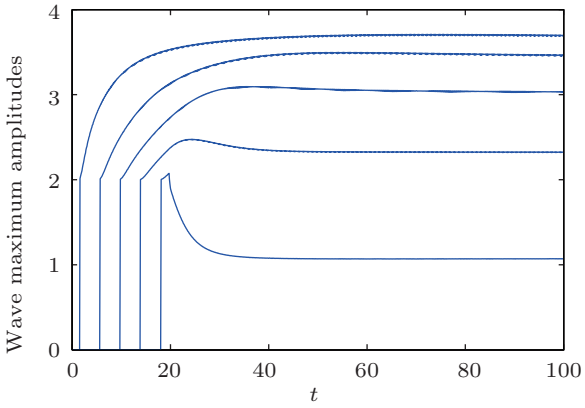


Fig. 5. (color online) The evolution of wave amplitudes.

Table 7. Solitary wave amplitude with $U_0=2$, $h=0.4$, $\Delta t=0.1$, $p=1$ and period of forcing $0\le t_0\le 20$, $0\le x\le 260$.

Time	1	2	3	4	5	C_1	C_2	C_3
2.5	2.26					8.9397	16.1942	74.8986
5	2.78					19.3958	41.3363	206.5459
7.5	3.05	2.24				29.3109	64.3064	324.6697
10	3.23	2.53	2.02			39.2124	87.2152	442.2752
15	3.44	2.91	2.43	2.06		59.2209	133.8372	682.1665
20	3.53	3.14	2.73	2.38	1.90	76.8502	175.1059	882.7008
40	3.67	3.46	3.08	2.35	1.08	78.5060	174.3022	882.6289
60	3.70	3.50	3.05	2.33	1.07	78.4275	173.5305	877.6376
80	3.70	3.48	3.03	2.33	1.07	78.3394	172.7643	872.6609
100	3.68	3.47	3.03	2.32	1.07	78.2589	172.0094	867.7610
100[31]	3.76	3.52	3.06	2.33	1.07			
100[20]	3.77	3.52	3.08	2.38	1.18			
100[32]	3.76	3.51	3.07	2.31	0.98			

4. Conclusion

In this paper, we investigated the utility of the exponential B-spline algorithm for solving the RLW equation. The efficiency of the method is tested on the propagation of the single solitary wave, the interaction of two solitary waves and wave generation. To see the accuracy of the method, L_∞ error norm and conservation quantities C_1, C_2 and C_3 are documented based on the obtained results. Exponential B-spline based method gives accurate and reliable results for solving the RLW equation. For the first test problem, generally EBSGM leads to more accurate results than the collocation-based methods but similar results with the some Galerkin methods.

In the second test problem, there is no exact solution therefore simulation is shown graphically and the conservation quantities are tabulated. Generation of waves by using variable boundary conditions at left has been achieved and wave profiles and their amplitudes are documented. In conclude, the numerical algorithm in which the exponential B-spline functions are used, performs well compared with other existing numerical methods for the solution of RLW equation.

Acknowledgment

This paper was presented at the 20th International Conference on Mathematical Modelling and Analysis (MMA2015) in Sigulda, Latvia.

References

[1] Peregrine D H 1966 *J. Fluid. Mech.* **25** 321
[2] McCartin B J 1991 *J. Approx. Theory* **66** 1
[3] Sakai M and Usmani R A 1989 *Numer. Math.* **55** 493
[4] Radunovic D 2008 *Numer. Algor.* **47** 191
[5] Rao S C S and Kumar M 2008 *Appl. Numer. Math.* **59** 1572
[6] Mohammadi R 2013 *Appl. Math.* **4** 933
[7] Dag I and Ersoy O 2015 *AIP Conf. Proc.* **1648** 370008
[8] Dag I and Ersoy O 2016 *Chaos, Solitons and Fractals* **86** 101
[9] Mohammadi R 2015 *Chin. Phys. B* **24** 050206
[10] Zorsahin Gorgulu M, Dag I and Irk D 2016 *J. Phys.: Conf. Ser.* **766** 012031
[11] Jain P J and Iskandar L 1979 *Comput. Meth. Appl. Mech. Eng.* **20** 195
[12] Jain P C, Shankar R and Singh T V 1993 *Commum. Numer. Methods Eng.* **9** 579–586
[13] Bhardwaj D and Shankar R 2000 *Comput. Math. Appl.* **40** 1397
[14] Kutluay S and Esen A 2006 *Math. Probl. Eng.* **2006** 85743
[15] Alexander M E and Morris J L 1979 *J. Comput. Phys.* **30** 428
[16] Sanz-Serna J M and Petrov I C 1981 *J. Comput. Phys.* **39** 94
[17] Luo Z and Liu R 1998 *SIAM. J. Numer. Anal.* **36** 89
[18] Dag I, Saka B and Irk D 2004 *Appl. Math. Comput.* **159** 373
[19] Saka B and Dag I 2008 *Commun. Numer. Method En.* **24** 1339
[20] Saka B, Dag I and Dogan A 2004 *Int. J. Comput. Math.* **81** 727
[21] Dag I and Ozer M N 2001 *Appl. Math. Model.* **25** 221
[22] Dag I, Saka B and Irk D 2006 *Comput. Appl. Math.* **190** 532
[23] Dag I, Dogan A and Saka B 2003 *Int. J. Comput. Math.* **80** 743
[24] Avilez-Valente P and Seabra-Santos F J 2004 *Int. J. Comput. Math.* **34** 256
[25] Mei L and Chen Y 2012 *Comput. Phys. Commun.* **183** 1609
[26] Guo B and Cao W 1988 *J. Comput. Phys.* **74** 110
[27] Sloan D M 1991 *J. Comput. Appl. Math.* **36** 159
[28] Ben-Yu G and Manoranjan V S 1985 *IMA J. Numer. Anal.* **5** 228
[29] Benjamin T B, Bona J L and Mahony J J 1972 *Phil. Trans. Roy. Soc.* **272** 47
[30] Olver P J 1979 *Math. Proc. Camb. Phil. Soc.* **85** 143
[31] Gardner L R T and Dag I 1995 *Il Nuovo Cimento B* **110** 1487
[32] Chang Q, Wang G and Guo B 1991 *J. Comput. Phys.* **93** 360